JOURNAL OF OCULAR PHARMACOLOGY AND THERAPEUTICS
Volume 34, Number 3, 2018

DOI: 10.1089/jop.2017.0094

Topical Glycyrrhizin Is Therapeutic for *Pseudomonas aeruginosa* Keratitis

Sandamali A. Ekanayaka, Sharon A. McClellan, Ronald P. Barrett, and Linda D. Hazlett

Abstract

Purpose: Glycyrrhizin (GLY), an inhibitor of high-mobility group box 1 (HMGB1) protects prophylactically against *Pseudomonas aeruginosa* keratitis. However, the therapeutic potential of GLY to enhance an antibiotic has not been tested and is our purpose.
Methods: C57BL/6 mice (B6) were infected with a clinical isolate (KEI 1025) of *P. aeruginosa* and treated topically at 6 h postinfection (p.i.) with GLY or phosphate-buffered saline (PBS). Clinical scores, photography with a slit lamp, enzyme-linked immunosorbent assay, myeloperoxidase assay, bacterial plate counts, histopathology, reactive oxygen/nitrogen species (ROS/RNS) assays, and *in vitro* macrophage (Mϕ) stimulation assays were used to assess effects of GLY treatment. In separate similar experiments, the ability of GLY to bioenhance the antibiotic, tobramycin (TOB), was assessed.
Results: *In vivo*, GLY versus PBS topical treatment began at 6 h p.i., improved disease outcome by significantly reducing clinical scores, proinflammatory proteins (HMGB1, RAGE, TLR4, TNF-α, and CXCL2), neutrophil infiltrate, bacterial load, ROS/RNS, and nitric oxide. *In vitro*, GLY downregulated iNOS and COX-2 expression (mRNA) in both mouse and human (THP-1) Mϕ. At 6 and 24 h p.i., treatment with GLY enhanced the effects of TOB compared with TOB alone by significantly reducing corneal bacterial load and/or protein levels of cytokines CXCL2 and IL-1β.
Conclusions: Data provide evidence that GLY is not only therapeutic for Pseudomonas keratitis through its ability to reduce HMGB1, bacterial load, and oxidative damage but also through its bioenhancement of an antibiotic, even when treatment is initiated at 24 h after infection.

Keywords: glycyrrhizin, keratitis, Pseudomonas, HMGB1, mice, topical treatment

Introduction

PSEUDOMONAS AERUGINOSA, an opportunistic gram-negative pathogen, is one of the most virulent organisms associated with microbial keratitis worldwide.[1–3] Currently, antibiotics are used to treat this disease, but with the global emergence of multidrug-resistant *P. aeruginosa* strains, alternative therapies are an urgent need.[4,5]

In this regard, recently we showed that extracellular high-mobility group box 1 (HMGB1), a late mediator of the inflammatory response,[6,7] provides a target for intervention in Pseudomonas keratitis.[8–10] Using a susceptible mouse model, we demonstrated prophylactic treatment strategies such as gene silencing, antibody neutralization, or use of glycyrrhizin (GLY) decreases HMGB1 levels, improving disease outcome.[9,10] However, prophylaxis has little relevance to clinical treatment of keratitis. For instance gene silencing has both toxicity and longevity issues.[11,12] Moreover, subconjunctival and systemic drug administration routes utilized in these prophylactic studies have side effects if used clinically.[13–15] These include anxiety, pain, conjunctival scarring, subconjunctival hemorrhage, and increased systemic drug toxicity.[13,15]

Thus, to overcome these limitations, the current study investigated the therapeutic efficacy of topical GLY treatment in susceptible B6 mice.[9,16] We provide *in vivo* evidence that GLY treatment began at 6 h postinfection (p.i.) significantly downregulates HMGB1 protein, decreases the neutrophil infiltrate, bacterial plate count, and reactive oxygen/nitrogen species (ROS/RNS) in the infected cornea. *In vitro* GLY also downregulates mRNA levels of ROS/RNS generating cytokines, iNOS, and COX-2 in lipopolysaccharide (LPS)-stimulated mouse and human Mϕ. GLY also bioenhanced the

Department of Anatomy and Cell Biology, Wayne State University School of Medicine, Detroit, Michigan.

effects of tobramycin (TOB),[17] an antibiotic used clinically to treat Pseudomonas keratitis. Collectively, this study provides evidence that GLY topical treatment is protective, has potential therapeutic value, and enhances antibiotic efficacy, all relevant to clinical management of keratitis.

Methods

Mice

Eight-week-old female C57BL/6 (B6) mice (Jackson Laboratory, Bar Harbor, ME) were housed in accordance with the National Institutes of Health guidelines. Mice were treated humanely and in compliance with the Association for Research in Vision and Ophthalmology Statement for the Use of Animals in Ophthalmic and Vision Research and the Institutional Animal Care and Use Committee of Wayne State University.

Bacterial culture and infection

P. aeruginosa strain, KEI 1025, a noncytotoxic clinical isolate strain expressing *exoT* and *exoS*[18] (Kresge Eye Institute, Detroit, MI) was grown in peptone tryptic soy broth medium in a rotary shaker water bath at 37°C and 150 rpm for 18 h to an optical density (measured at 540 nm) between 1.3 and 1.8. Bacterial cultures were centrifuged at 5,500 *g* for 10 min, pellets washed once with sterile saline, recentrifuged, resuspended, and diluted in sterile saline. Anesthetized mice were placed beneath a stereoscopic microscope at 40× magnification. The left cornea was scarified, and 5 μL containing 1×10^7 colony-forming units (CFU)/μL of the bacterial suspension was applied topically.

Ocular response to bacterial infection

A disease grading scale[19] was used to assign a clinical score to each infected eye. Clinical scores were designated as follows: 0 = clear or slight opacity, partially or fully covering the pupil; +1 = slight opacity, fully covering the anterior segment; +2 = dense opacity, partially or fully covering the pupil; +3 = dense opacity, covering the entire anterior segment; and +4 = corneal perforation or phthisis. Clinical scores to compare disease severity were accompanied by photographs taken using a slit lamp.

GLY topical treatment

Infected eyes of B6 mice ($n=5$/group/time) were treated topically (5 μL of each agent/time point) with 20 μg/μL GLY (Cat. No. 5053;, Sigma-Aldrich, St. Louis, MO) or sterile phosphate-buffered saline (PBS; control). GLY concentration was chosen based on published reports.[10,20,21] Topical treatment times tested (6 or 8 h p.i.) were followed by treatment twice daily from 1 to 4 days p.i. as described above.

GLY combined treatment with TOB

At 6 h p.i., infected eyes of B6 mice ($n=5$/group/time) were treated topically with 5 μL of sterile PBS, 20 μg/μL GLY and 1.5 mg/mL TOB (Alcon, Ft. Worth, TX) ±20 μg/μL GLY. In a separate experiment, topical treatment was begun at 24 h p.i. and KEI 1025 infected eyes of B6 mice ($n=10$/group/time) were treated twice daily for 2 days with 5 μL PBS or 1.5 mg/mL TOB ±20 μg/μL GLY.

Enzyme-linked immunosorbent assay

PBS- or GLY-treated B6 mice ($n=5$/group/time) were sacrificed at 3 and 5 days p.i. and corneas (normal and infected) harvested to test HMGB1, TLR4, RAGE, TNF-α, and CXCL2 expression. In a separate experiment, PBS- or TOB ± GLY-treated B6 mice ($n=5$/group/time) were sacrificed at 2 and 3 days p.i. and normal and infected corneas harvested to test protein expression of CXCL2 and IL-1β. To quantify HMGB1, TLR4, RAGE, TNF-α, and IL-1β proteins, individual corneas were homogenized in 500 μL of PBS containing 0.1% Tween 20 (Sigma-Aldrich) and protease inhibitors (Roche, Indianapolis, IN). For CXCL2, individual corneas were homogenized in 1 mL of 50 mM potassium phosphate buffer (pH 6.0) containing 0.5% hexadecyltrimethylammonium bromide (HTAB; Sigma-Aldrich) and protease inhibitors.

Corneal homogenates were centrifuged at 12,000 *g* for 10 min. A 50 μL aliquot of each supernatant was assayed in duplicate to quantify proteins using enzyme-linked immunosorbent assay (ELISA) kits: HMGB1 (Chondrex, Inc., Redmond, WA), TLR4 (MyBioSource, Inc., San Diego, CA), RAGE (R&D Systems, Minneapolis, MN), TNF-α (R&D Systems), CXCL2 (R&D Systems), and IL-1β (R&D Systems). Undiluted supernatant aliquots were used to quantify all proteins except HMGB1 (1:5 dilution), RAGE (1:2 dilution), and CXCL2 (1:5 dilution); assays were run following the manufacturer's instructions. Sensitivities were as follows: 0.8 ng/mL (HMGB1), 2.36 pg/mL (RAGE), 1 pg/mL (TLR4), 1.88 pg/mL (TNF-α), 1.5 pg/mL (CXCL2), and 2.31 pg/mL (IL-1β).

Myeloperoxidase assay

This assay was used to quantitate neutrophils in the infected cornea of GLY and PBS-treated mice ($n=5$/group/time). Individual corneas were removed at 3 and 5 days p.i. and homogenized in 1 mL of 50 mM phosphate buffer (pH 6.0) containing 0.5% HTAB. Samples were freeze-thawed 4 times, and after centrifugation, 100 μL of the supernatant was added to 2.9 mL of 50 mM phosphate buffer containing *o*-dianisidine dihydrochloride (16.7 mg/mL; Sigma-Aldrich) and hydrogen peroxide (0.0005%). Change in absorbance was monitored at 460 nm for 5 min at 30 s intervals; the slope of the line was determined for each sample and units of myeloperoxidase (MPO)/cornea calculated. One unit of MPO activity is equivalent to $\sim2\times10^5$ neutrophils.[22]

Quantification of viable bacteria

Mice were sacrificed at 1, 3, and 5 days p.i. and GLY- or PBS-treated infected corneas were harvested ($n=5$/group/time). Untreated corneas from each group also were harvested from mice ($n=5$/group/time) at 6 h p.i. Each cornea was homogenized in 1 mL of sterile saline (0.85% NaCl, pH 7.4) containing 0.25% BSA. A 100 μL of the homogenate was serially diluted (1:10) in sterile saline containing 0.25% BSA. Selected dilutions were plated in triplicate on selective culture medium (Difco™ Pseudomonas Isolation Agar; BD Biosciences, Inc., Franklin Lakes, NJ). Plates were incubated overnight at 37°C and viable bacteria counted. In the first of 2 similar, separate experiments, plate counts were performed at 1 day p.i. following treatment of infected eyes at 6 h p.i. with PBS, GLY, or TOB±GLY ($n=5$/group/time).

In the second, plate counts were done at 2 and 3 days p.i. after initiating treatment at 24 h p.i. with PBS or TOB±GLY,

using a similar number of animals. Results are reported as $\log_{10}$ CFU/cornea ± standard error of the mean (SEM).

Histopathology

Infected eyes ($n = 3$/group/time) were enucleated from GLY-, PBS-, and TOB±GLY-treated mice at 3 and/or 5 days p.i., immersed in PBS, rinsed, and fixed in 1% osmium tetroxide [Electron Microscopy Sciences (EMS), Hatfield, PA], 2.5% glutaraldehyde (EMS), and 0.2 M Sorenson's phosphate buffer (pH 7.4; Sigma-Aldrich) at 4°C for 3 h. Eyes were rinsed with 0.1 M phosphate buffer, dehydrated in ethanols and propylene oxide (Sigma-Aldrich), and infiltrated and embedded in Epon-Araldite (EMS). Sections (1.5 μm) were cut, stained with Richardson's stain, and photographed (Leica DM4000B; Leica Microsystems, Inc.), as described before.[23]

Isolation and stimulation of mouse and human macrophages (Mϕ)

Mouse peritoneal Mϕ were isolated from B6 mice as described before.[24,25] In brief, Mϕ were induced into the peritoneal cavity by intraperitoneal injection of 1 mL of 3% Brewer's thioglycollate medium (BD Biosciences, Sparks, MD) 5 days before harvest. Cells were collected by peritoneal lavage with DMEM containing 10% heat-inactivated fetal bovine serum (FBS; Invitrogen Life Technologies, Carlsbad, CA), penicillin (100 U/mL; Invitrogen), and streptomycin (100 μg/mL; Invitrogen) and stained with 0.4% trypan blue and viable cells (>95%) counted with a hemacytometer. Mϕ were seeded (1 mL/well) at a density of 2×10^6 cells/well ($n = 5$wells/group) and incubated for 4 h.

In a separate experiment, human THP-1 cells [American Type Culture Collection (ATCC), Manassas, VA] were grown per the company's instructions. 1×10^6 cells/well ($n = 5$wells/group) were differentiated from the monocyte-like state into Mϕ. For this, cells were treated for 72 h with 100 ng/mL phorbol 12-myristate 13-acetate (PMA; Sigma-Aldrich) and differentiated adherent cells exhibiting Mϕ-like morphology were washed once with sterile PBS. Cells were incubated with RPMI 1640 medium without PMA, containing 10% FBS, penicillin, (100 U/mL) and streptomycin (100 μg/mL) for 24 h at 37°C. Both groups of Mϕ were washed once with growth medium (DMEM or RPMI 1640), treated with ±2 mM GLY (in growth medium) and stimulated with LPS (*P. aeruginosa* serotype 10; Sigma-Aldrich) (1 μg/mL) or ultrapure LPS (1 μg/mL, specific for TLR4; InvivoGen, San Diego, CA) for 18 h at 37°C. In a separate similar experiment, human macrophages were incubated for 3 h with 10 multiplicity of infection (MOI) KEI 1025. Unstimulated Mϕ treated with growth medium ±2 mM GLY and incubated for 18 h at 37°C served as the negative control.

Real time reverse transcription-polymerase chain reaction (RT-PCR)

Mϕ (mouse peritoneal or human THP-1 cells) were washed once with PBS and total RNA isolated using RNA STAT-60™ (Tel-Test, Friendswood, TX) per the manufacturer's instructions. After spectrophotometric quantification at 260 nm, 1 μg of each RNA sample was reverse transcribed using Moloney murine leukemia virus reverse transcriptase (Invitrogen) to produce a cDNA template for polymerase chain reaction (PCR). cDNA products were diluted 1:25 with diethylpyrocarbonate-treated water. A 2 μL aliquot of diluted cDNA was used for the PCR with Real-Time SYBR® Green/Fluorescein PCR Master Mix (Bio-Rad, Richmond, CA) and primer concentrations of 10 μM (10 μL total volume). After a preprogrammed hot-start cycle (3 min at 95°C), the parameters used for PCR amplification were as follows: 15 s at 95°C and 60 s at 60°C with the cycles repeated 45×. Conditions for PCR amplification of cDNA were established using routine methods.[9,26] mRNA levels of mouse or human iNOS and COX-2 were tested by PCR (CFX Connect™ Real-Time PCR Detection System; Bio-Rad). Fold differences in gene expression were calculated after normalization to β-actin (mouse Mϕ) or GAPDH (human THP-1 Mϕ) and expressed as relative mRNA concentration ± SEM. The primer pair sequences used for PCR are shown (Table 1).

Measurement of corneal ROS/RNS levels

ROS/RNS levels in the cornea were measured using an OxiSelect™ *in vitro* ROS/RNS Assay Kit (Cell Biolabs, Inc., San Diego, CA) per manufacturer's instructions. In this assay, a ROS/RNS specific, nonfluorescent 2′, 7′-dichlorodihydrofluorescein (DCFH) reacts with ROS/RNS

Table 1. Nucleotide Sequence of the Specific Primers Used for Polymerase Chain Reaction Amplification

Gene	*Nucleotide sequence*	*Primer*	*GenBank*
mβ-actin	5′-GAT TAC TGC TCT GGC TCC TAG C-3′	F	NM_007393.3
	5′-GAC TCA TCG TAC TCC TGC TTG C-3′	R	
miNOS	5′-TCC TCA CTG GGA CAG CAC AGA ATG-3′	F	NM_010927.3
	5′-GTG TCA TGC AAA ATC TCT CCA CTG CC-3′	R	
mCOX2	5′-TGC ACT ATG GTT ACA AAA GCT GG-3′	F	NM_011198.3
	5′-TCA GGA AGC TCC TTA TTT CCC TT-3′	R	
hGAPDH	5′-GGA GCG AGA TCC CTC CAA AAT-3′	F	NM_002046.4
	5′-GGC TGT TGT CAT ACT TCT CAT GG-3′	R	
hiNOS	5′-CAT CCT CTT TGC GAC AGA GAC-3′	F	NM_000625.3
	5′-GCA GCT CAG CCT GTA CTT ATC-3′	R	
hCOX2	5′-CAG CAC TTC ACG CAT CAG TT-3′	F	NM_000963.2
	5′-CGC AGT TTA CGC TGT CTA GC-3′	R	

F, forward; *h*, human; *m*, mouse; R, reverse.

species, generating a highly fluorescent molecule 2,7 dichlorodihydrofluorescein (DCF). Fluorescence intensity of DCF (Excitation 480 nm/Emission 530 nm) was proportional to the total ROS/RNS levels in the unknown sample and ROS/RNS content was determined compared with known DCF standards. For this assay, PBS- or GLY-treated B6 mice ($n = 5$/group/time) were sacrificed at 3 and 5 days p.i. and corneas (normal and infected) harvested. Corneas were homogenized in 500 μL of cold PBS and centrifuged at 10,000 *g* for 5 min. A 50 μL aliquot of each supernatant was added to a 96-well black microtiter plate in duplicate and incubated with 50 μL of catalyst for 5 min and followed by incubation with 100 μL DCFH for 30 min. DCF fluorescence was measured and total ROS/RNS concentration (nM/cornea) in corneal homogenates determined. Results = total ROS/RNS concentration ± SEM.

Griess assay

Nitric oxide (NO) production in the cornea was measured using Griess reagent (Sigma-Aldrich). Infected GLY- or PBS-treated mice ($n = 5$/group/time) were sacrificed at 3 and 5 days p.i. and normal and infected corneas harvested. Corneal samples were homogenized in 500 μL of sterile, degassed PBS and centrifuged at 3,500 rpm for 5 min. One hundred microliters aliquots were incubated with 100 μL of Griess reagent for 15 min at room temperature. Absorbance was measured at 570 nm and nitrite concentration calculated using a sodium nitrite standard curve. The data are reported as nitrite concentration ± SEM.

Statistical analysis

The difference in clinical score between 2 groups was analyzed by the Mann–Whitney *U* test (GraphPad Prism, San Diego, CA). For comparison of 3 or more groups (plate count, ELISA), a one-way ANOVA followed by the Bonferroni's multiple comparison test (GraphPad Prism) was used. For all other experiments (ELISA, MPO, plate count, total ROS/RNS, and Griess assay), an unpaired, 2-tailed Student's *t*-test determined significance. For each test, $P \leq 0.05$ was considered significant; data are shown as mean ± SEM. Experiments were repeated at least once for reproducibility.

Results

Ocular response to GLY topical treatment

For topical GLY versus PBS, treatment was begun at 8 h p.i. (Fig. 1A–C), clinical scores (Fig. 1A) showed significantly reduced disease only at 3 ($P < 0.05$), but not at 5

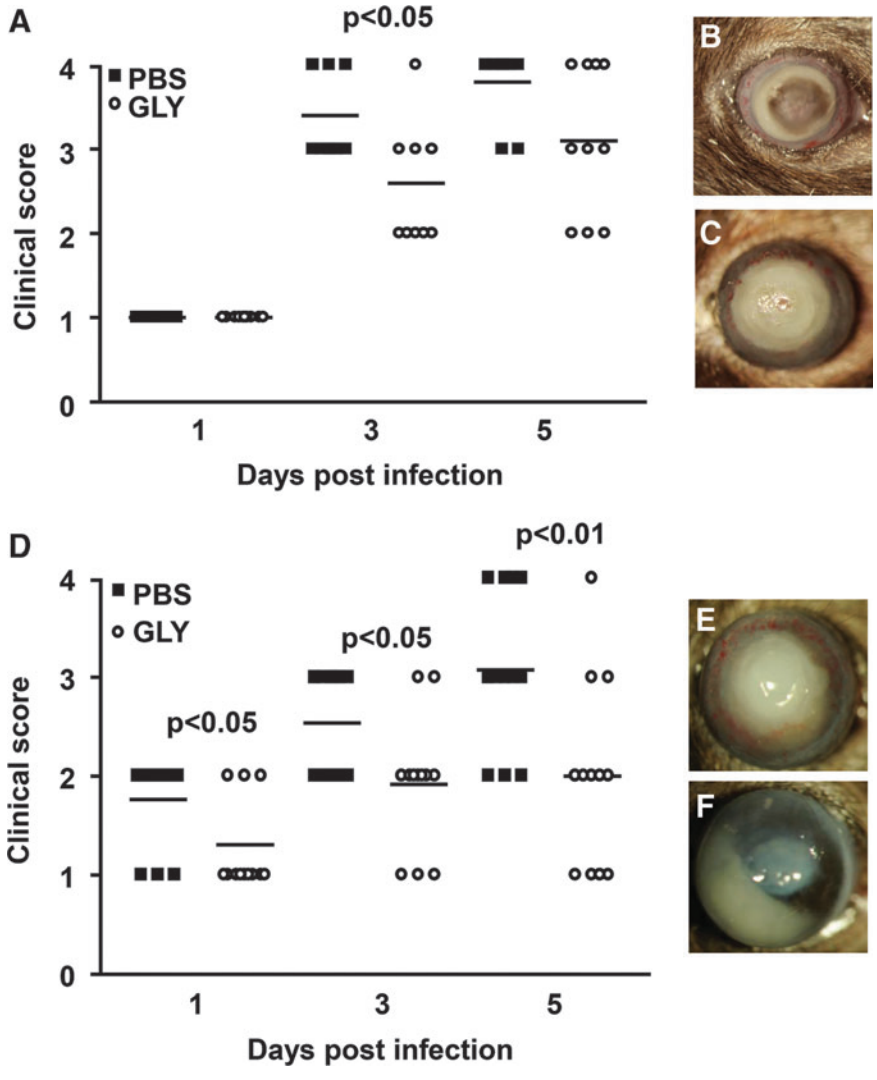

FIG. 1. Disease response: GLY topical treatment. For GLY versus PBS topical treatment begun at 8 h p.i., clinical scores **(A)** were reduced significantly only at 3 days p.i. No difference in clinical scores was seen between the groups at 1 and 5 days p.i. ($n = 10$/group/time). Photographs taken with a slit lamp at 5 days p.i. from PBS- **(B)** and GLY-treated **(C)** eyes of B6 mice illustrate the disease response. For treatment began at 6 h p.i., clinical scores **(D)** were reduced significantly at 1, 3, and 5 days p.i. ($n = 12$/group/time) after GLY. Photographs taken with a slit lamp at 5 days p.i. from PBS- **(E)** and GLY-treated **(F)** eyes confirmed reduction in opacity with less cellular infiltrate after GLY treatment. Data were analyzed using a nonparametric Mann–Whitney *U* test. Horizontal lines indicate median values. Magnification **(B, C)** = 8×. GLY, glycyrrhizin; PBS, phosphate-buffered saline; p.i., postinfection.

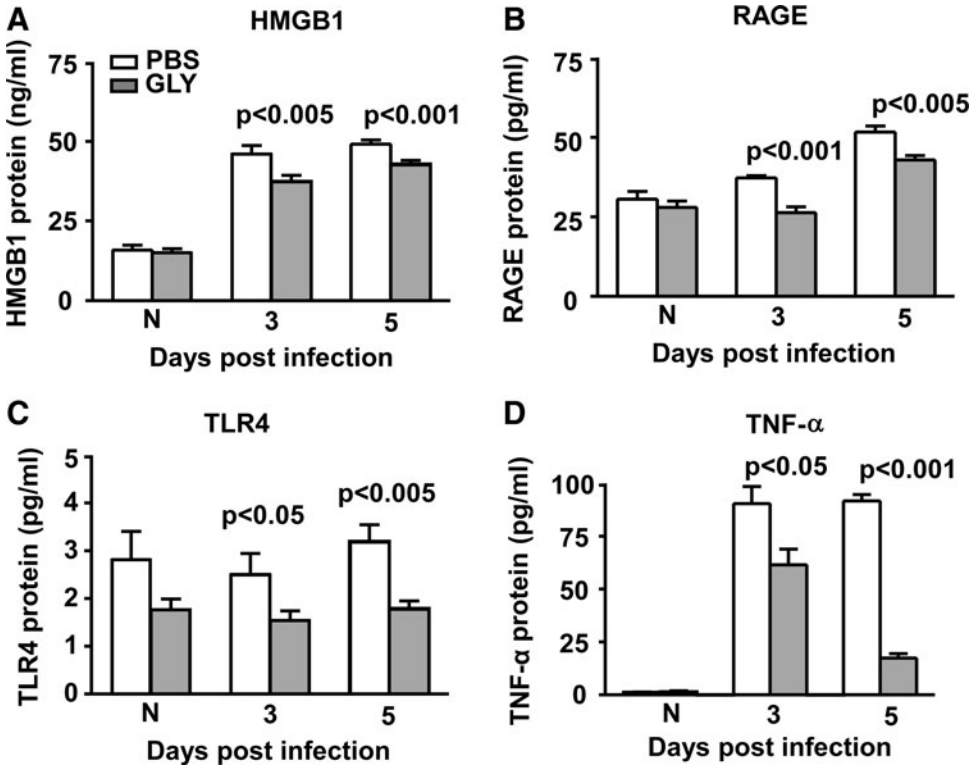

FIG. 2. HMGB1, RAGE, TLR4, and TNF-α ELISA: GLY topical treatment (6 h p.i.). Corneal protein levels of HMGB1 **(A)**, RAGE **(B)**, TLR4 **(C),** and TNF-α **(D)** were reduced significantly at 3 and 5 days p.i. after GLY versus PBS topical treatment. No difference in protein levels was seen between groups for normal uninfected (N) cornea **(A–D)**. All data are mean ± SEM and were analyzed using a 2-tailed Student's *t*-test ($n = 5$/group/time). ELISA, enzyme-linked immunosorbent assay; HMGB1, high-mobility group box 1; SEM, standard error of the mean.

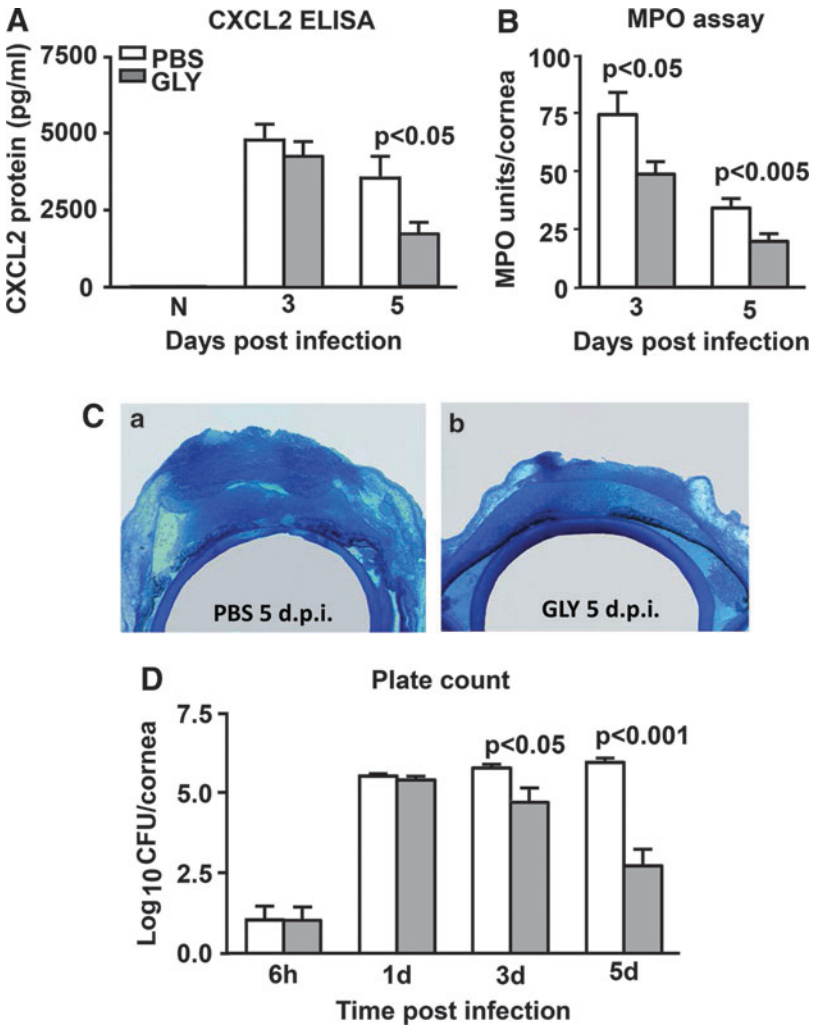

FIG. 3. CXCL2 ELISA, MPO assay, histopathology and plate count: GLY topical treatment (6 h p.i.). Corneal protein levels of CXCL2 **(A)** were reduced significantly only at 5 days p.i. after GLY treatment with no difference between groups at 3 days p.i. or in normal uninfected (N) cornea. MPO levels **(B)** were reduced significantly at 3 and 5 days p.i. in the infected, GLY- versus PBS-treated cornea. After GLY treatment, bacterial plate counts **(D)** were reduced significantly only at 3 and 5 days p.i. with no difference at 6 h or 1 day p.i. All data are mean ± SEM and were analyzed using a 2-tailed Student's *t*-test ($n = 5$/group/time). Histopathology **(C-a, b)** revealed a heavy cellular infiltrate in the stroma and anterior chamber of PBS-treated eye at 5 days p.i. **(C-a)**. The eyes of GLY-treated **(C-b)** mice showed fewer infiltrated cells into cornea and anterior chamber, and less edema, at 5 days p.i. Magnification **(C-a, b)** = 30×, $n = 3$/group/time. MPO, myeloperoxidase.

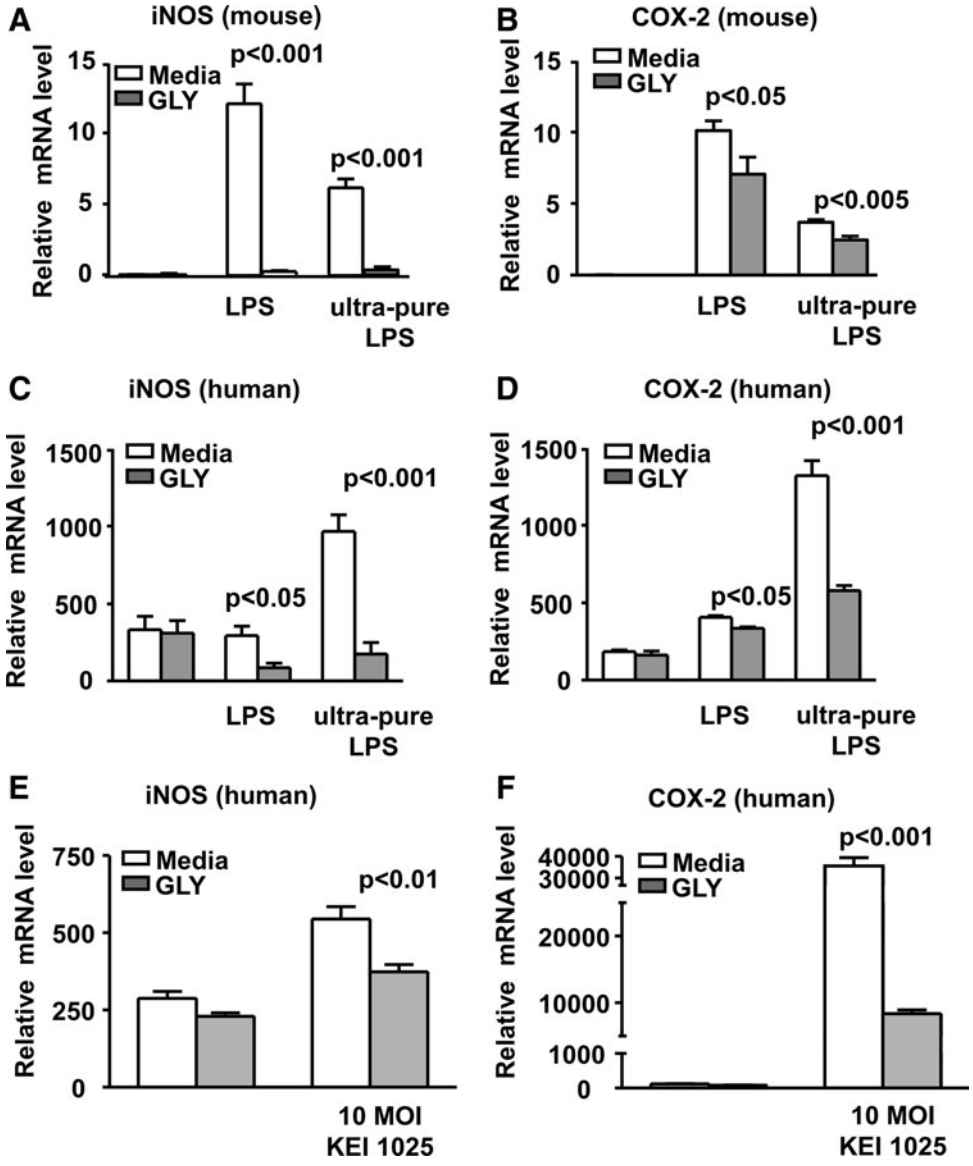

FIG. 4. Effects of GLY on modulation of oxidative stress *in vitro*. Real-time reverse transcription-PCR showed significantly reduced mRNA expression for iNOS **(A)** and COX-2 **(B)** after GLY treatment in LPS or ultrapure LPS-stimulated mouse peritoneal Mϕ. For LPS or ultrapure LPS stimulated, GLY-treated human THP-1 Mϕ, relative mRNA levels were also reduced significantly for iNOS **(C)** and COX-2 **(D)**. Human THP-1 Mϕ incubated with 10 MOI KEI 1025 showed significant reduction in mRNA levels of iNOS **(E)** and COX-2 **(F)** after GLY treatment. No difference in relative mRNA levels was seen for unstimulated, GLY- versus media-treated mouse and human Mϕ. All data are mean ± SEM and were analyzed using a 2-tailed Student's *t*-test ($n = 5$/group/time). LPS, lipopolysaccharide; MOI, multiplicity of infection; PCR, polymerase chain reaction.

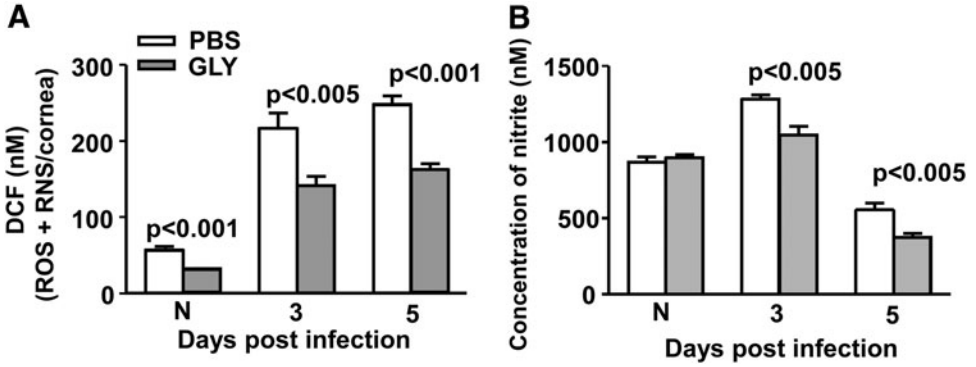

FIG. 5. Effects of GLY on modulation of oxidative stress *in vivo*. GLY versus PBS topical treatment significantly reduced total ROS/RNS **(A)** concentration in the uninfected normal cornea (N) and the infected cornea at 3 and 5 days p.i. Corneal nitrite levels **(B)** were also reduced significantly in the GLY- versus PBS-treated infected cornea at 3 and 5 days p.i. Nitrite levels were not different in the uninfected normal cornea (N) between the groups. All data are mean ± SEM and were analyzed using a 2-tailed Student's *t*-test ($n = 5$/group/time). ROS/RNS, reactive oxygen/nitrogen species.

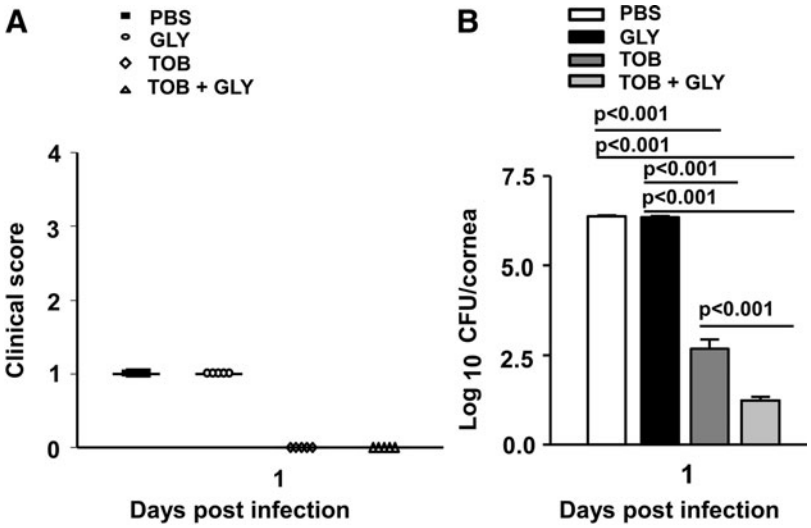

FIG. 6. Disease response and plate count: TOB±GLY topical treatment at 6 h p.i Clinical scores **(A)** were not significantly different between treatment groups (PBS, GLY, TOB±GLY) at 1 day p.i. Viable bacterial load **(B)** was reduced significantly at 1 day p.i. for TOB+GLY versus TOB alone and TOB±GLY versus PBS or GLY groups. No difference in bacterial plate count was seen for GLY versus PBS at 1 day p.i. Clinical score data were analyzed using a nonparametric Mann–Whitney *U* test. Horizontal lines indicate the median values. $n = 5$/group/time. Plate count data are shown as mean ± SEM and were analyzed using one-way ANOVA followed by the Bonferroni's multiple comparison test. $n = 5$/group/time. TOB, tobramycin.

($P = 0.09$) days p.i. ($n = 10$ mice/group/time). Photographs taken with a slit lamp (Fig. 1B, PBS and C, GLY) at 5 days p.i. illustrate the lack of protection for this treatment time. However, the infected corneas of GLY-treated mice, began at 6 h p.i., exhibited significantly less disease and lower clinical scores (Fig. 1D) than PBS-treated mice ($n = 12$ mice/group/time), at 1 ($P < 0.05$), 3 ($P < 0.05$), and 5 ($P < 0.01$) days p.i. Photographs taken with a slit lamp of representative eyes from PBS- (Fig. 1E) and GLY-treated (Fig. 1F) mice at 5 days p.i. depict reduced opacity after GLY treatment.

GLY topical treatment effects proinflammatory molecules

The above studies established that a 6 h p.i. time window was optimum for treating with GLY, and thus was studied further. GLY versus PBS treatment downregulated HMGB1 protein expression (Fig. 2A) significantly at 3 ($P < 0.005$) and 5 ($P < 0.001$) days p.i. Protein expression of other proinflammatory molecules, including RAGE (Fig. 2B: $P < 0.001$ and $P < 0.005$ at 3 and 5 days p.i.), TLR4 (Fig. 2C: $P < 0.05$ and $P < 0.005$ at 3 and 5 days p.i.), and TNF-α (Fig. 2D: $P < 0.05$ and $P < 0.001$ at 3 and 5 days p.i.) also were significantly downregulated in the GLY versus PBS group. Protein levels did not differ significantly in normal (N) corneas for either group (Fig. 2A–D).

Similar GLY treatment reduced the inflammatory environment

GLY treatment significantly decreased CXCL2 protein expression (Fig. 3A) only at 5 ($P < 0.05$) days p.i. CXCL2 protein was not detected in the uninfected normal (N) cornea and was reduced slightly but not significantly at 3 days p.i. after GLY treatment. An MPO assay (Fig. 3B) revealed significantly reduced levels of neutrophils in the GLY- versus PBS-treated cornea at both 3 ($P < 0.05$) and 5 ($P < 0.005$) days p.i. Infected GLY- and PBS-treated eyes also were examined histologically (Fig. 3C). Reflective of the MPO data, GLY treatment markedly reduced the cellular infiltrate in the corneal stroma and anterior chamber of the infected eye at 5 days p.i. (Fig. 3C-b). In contrast, PBS-treated eyes displayed denudation of the epithelium, a heavier stromal infiltrate with degradation and edema at 5 days p.i. (Fig. 3C-a). Bacterial plate counts (Fig. 3D) were used to detect viable bacteria in the infected cornea after GLY or PBS treatment. GLY treatment revealed reduced bacterial load at day 3 ($P < 0.05$) and 5 ($P < 0.001$), but not at 1 day p.i. or at 6 h p.i. (before treatment initiated) compared with PBS (Fig. 3D).

GLY effects oxidative stress

In vitro studies tested the effects of GLY on mRNA expression of oxidative stress associated molecules, iNOS and COX-2 using LPS or ultrapure LPS-stimulated mouse and human Mϕ (Fig. 4A–D). For mouse peritoneal Mϕ, GLY significantly reduced iNOS (Fig. 4A: $P < 0.001$; for LPS and ultrapure LPS) and COX-2 (Fig. 4B: $P < 0.05$; LPS and $P < 0.005$; ultrapure LPS). GLY treatment also significantly reduced iNOS expression (Fig. 4C: $P < 0.05$; LPS and $P < 0.001$; ultrapure LPS) and COX-2 (Fig. 4D: $P < 0.05$; LPS and $P < 0.001$; ultrapure LPS) in human Mϕ. In addition, human Mϕ were incubated with 10 MOI of the bacteria and GLY significantly reduced mRNA levels of both iNOS (Fig. 4E: $P < 0.01$) and COX-2 (Fig. 4F: $P < 0.001$).

In vivo, GLY versus PBS topical treatment after infection significantly reduced total ROS/RNS in the cornea (Fig. 5A) at 3 ($P < 0.005$) and 5 ($P < 0.001$) days p.i. Total ROS/RNS levels also were reduced significantly in the uninfected, normal contralateral cornea ($P < 0.001$) in the GLY versus PBS group. Corneal nitrite levels (Fig. 5B) were reduced significantly in the GLY- versus PBS-treated infected cornea at 3 and 5 days p.i. ($P < 0.005$). Nitrite levels were not different in the normal (N) cornea between groups.

Effects of TOB±GLY topically at 6 or 24 h p.i

Figure 6 shows clinical scores (Fig. 6A) and bacterial plate counts (Fig. 6B) at 1 day p.i. where treatment began at 6 h p.i. At 1 day p.i., the infected corneas were clear (clinical score = 0) for TOB alone or TOB+GLY-treated groups compared with PBS or GLY alone (clinical score = +1). Viable bacterial plate counts (Fig. 6B) were reduced significantly for TOB+GLY versus TOB alone ($P < 0.001$), indicating GLY potentiated

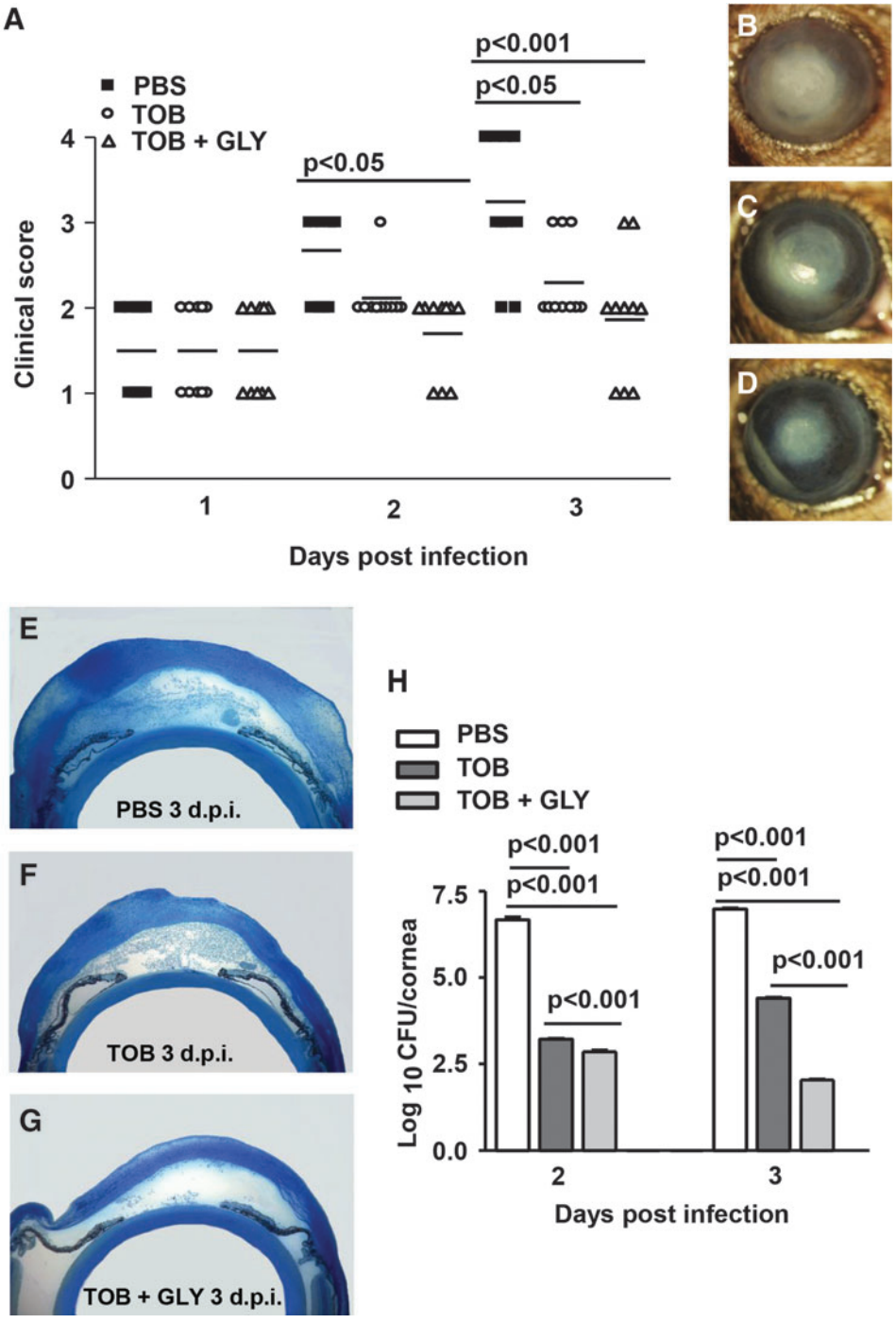

FIG. 7. Disease response and plate count: TOB±GLY topical treatment at 24 h p.i. At 2 and 3 days p.i., clinical scores **(A)** were reduced significantly only for the TOB+GLY versus PBS group. Photographs taken with slit lamp at 3 days p.i. **(B–D)** show reduced opacity in the TOB+GLY treated eyes **(D)** compared with PBS **(B)** or TOB alone **(C)**. Histopathology **(E–G)** revealed a heavy cellular infiltrate in the stroma and anterior chamber of PBS-treated eye at 3 days p.i. **(E)**. The eyes of TOB-treated **(F)** and TOB+GLY-treated **(G)** mice showed fewer infiltrated cells into cornea and anterior chamber, and less edema, at 3 days p.i., with best effects seen for the TOB+GLY-treated cornea. Magnification = 30×, $n = 3$/group/time. At 2 and 3 days p.i., viable bacterial load **(H)** was reduced significantly for TOB+GLY versus TOB alone and TOB±GLY versus PBS groups. Clinical score data were analyzed using a nonparametric Mann–Whitney *U* test. Horizontal lines indicate median values. Magnification **(B–D)** = 8×, $n = 10$/group/time. Plate count data are shown as mean ± SEM and were analyzed using one-way ANOVA followed by the Bonferroni's multiple comparison test. $n = 5$/group/time.

TOB effects. In addition, bacterial load after treatment with TOB alone or TOB+GLY was significantly reduced compared with PBS or GLY groups ($P < 0.001$ for all comparisons). When treatment was initiated at 24 h p.i. (Fig. 7A–H), clinical scores (Fig. 7A) were reduced significantly for the TOB+GLY-treated group ($P < 0.05$ at 2 and $P < 0.001$ at 3 days p.i.) compared with PBS. Significant differences also were seen when comparing TOB versus PBS ($P < 0.05$) at 3 days p.i. Clinical scores did not differ significantly between the other groups at all times. Photographs taken with a slit lamp (Fig. 7B–D) at 3 days p.i., showed less opacity in the TOB+GLY-treated eyes (Fig. 7D) compared with PBS (Fig. 7B) or TOB alone (Fig. 7C). Infected eyes also were examined histologically (Fig. 7E–G) after PBS or TOB±GLY. TOB±GLY treatment reduced the cellular infiltrate in the corneal stroma and anterior chamber of the infected eye at 3 days p.i. (Fig. 7F, G) and corneal edema when compared with PBS (Fig. 7E). When comparing TOB+GLY versus TOB alone, corneal edema and the anterior chamber infiltrate were minimal, agreeing with the photographs taken with a slit lamp. Viable bacterial load (Fig. 7H) was reduced significantly for TOB±GLY versus PBS at both 2 and 3 days p.i. ($P < 0.001$; for both). Load also was reduced significantly for TOB+GLY versus TOB alone at 2 and 3 days p.i. ($P < 0.001$). In a similar experiment, protein expression was reduced significantly for CXCL2 (Fig. 8A, $P < 0.001$) and IL-1β (Fig. 8B, $P < 0.001$) at 2 and 3 days p.i. for TOB±GLY versus PBS groups. For TOB+GLY versus TOB alone, protein expression was reduced significantly only at

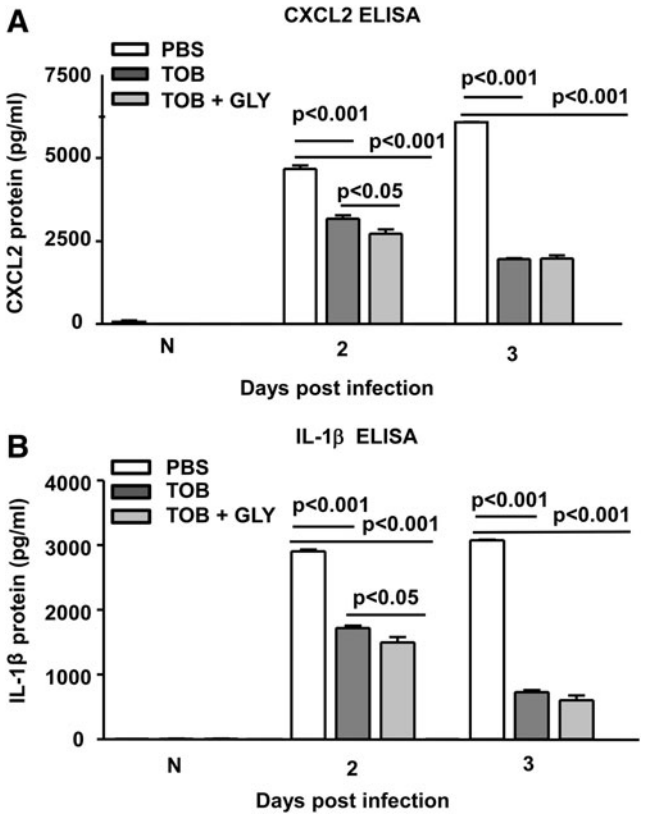

FIG. 8. CXCL2 and IL-1β ELISA: TOB±GLY topical treatment at 24 h p.i. Protein expression of CXCL2 **(A)** and IL-1β **(B)** was reduced significantly for the TOB±GLY versus PBS group at 2 and 3 days p.i. For the TOB+GLY versus TOB alone group, CXCL2 **(A)** and IL-1β **(B)** protein expression was reduced significantly only at 2 days p.i. For both proteins, no difference between groups was seen for TOB+GLY versus TOB alone at 3 days p.i. and for normal, uninfected (N) cornea. All data are mean ± SEM and were analyzed using a one-way ANOVA followed by the Bonferroni's multiple comparison test. $n = 5$/group/time.

2 days p.i. for CXCL2 (Fig. 8A, $P < 0.05$) and IL-1β (Fig. 8B, $P < 0.05$). No differences in expression of these proteins were detected in the normal (N), uninfected cornea.

Discussion

Currently, intensive antibiotic therapy with broad spectrum or fortified antibiotics is used to treat Pseudomonas keratitis, but with emergence of multidrug-resistant strains, alternative treatment strategies remain an urgent need.[27,28] Nonantibiotic therapies, including use of corticosteroids and phototherapy (corneal cross-linking)[5,13] have limitations, and their use clinically remains controversial. To approach this problem, we recently have shown that elevated levels of extracellular HMGB1, an alarmin, amplifies inflammation in *P. aeruginosa*-induced keratitis.[9] In the keratitis model, several strategies were used successfully to target HMGB1, including silencing and antibody neutralization.[9]

Use of small molecule inhibitors such as GLY or its derivatives, to attenuate HMGB1-mediated disease progression also have had success in prophylactic treatment of keratitis.[10] GLY is a natural compound that has been used with no adverse effects for treatment of diseases in other animal models,[29–32] as well as clinically in chronic hepatitis,[33] and blepharitis.[20] Its 18-β glycyrrhetinic acid moiety directly binds HMGB1, inhibiting extracellular secretion and proinflammatory effects.[34]

Since prophylactic studies have little clinical applicability,[9,10] but do provide proof of principle to guide therapeutic testing, we first determined how long after infection could topical treatment with GLY be delayed (6 and 8 h tested). Although 8 h was not protective, treatment initiated at 6 h p.i. significantly reduced corneal disease (clinical score) as well as HMGB1 protein expression. These data are consistent with other studies using GLY administered by various routes (e.g., systemic) that also showed reduced expression of HMGB1.[10,32,35–39] This confirms the ability of GLY to overcome drug delivery barriers to downregulate HMGB1 expression, regardless of the administration route.

HMGB1 has a myriad of functions and is involved in autocrine and paracrine positive feedback mechanisms, which sustain inflammation and contribute to disease pathogenesis.[40] For instance, it interacts with Toll-like receptors (TLRs) and RAGE activating downstream inflammatory cascades[6,40,41] leading to activation of NFκB, which upregulates expression of proinflammatory mediators, including TLRs and RAGE. This is due to the presence of NFκB-binding sites on the promotor regions of those receptors.[40]

In addition, it also has been reported that there is a proinflammatory feedback loop between HMGB1 and TNF-α which sustains inflammation.[40,42] Keeping this scenario in mind, we also tested and found that GLY therapy could modify HMGB1-mediated upregulation of RAGE, TLR4, and TNF-α. These data are consistent with *in vitro* studies by Zhao et al.,[39] using rat alveolar macrophage NR8383 cells (stimulated with LPS or HMGB1), who found that GLY treatment reduced interaction between HMGB1, RAGE, and TLR4.

Neutrophils are the predominate infiltrating cells in *P. aeruginosa* keratitis. They function to phagocytize and kill invading microorganisms, but their persistence contributes to disease pathogenesis.[43] HMGB1 triggers neutrophil-mediated inflammation and tissue damage via TLR and RAGE-mediated pathways.[44,45] In addition, during *P. aeruginosa* keratitis, activated corneal cells (epithelial and fibroblasts) produce chemoattractant cytokines, including CXCL2 and CXCL5, which together recruit neutrophils to the corneal stroma.[46] In this study, GLY topical treatment after infection reduced protein expression of CXCL2 and, in turn, neutrophil infiltration. This provides evidence that GLY can modulate the infiltration of these cells, even when therapy is delayed versus given prophylactically.[10]

During inflammation, Mϕ are the main source of NO[43] and PGE2.[47] In Mϕ, iNOS produces NO from L-arginine, using NADPH and O_2, while COX-2 converts arachidonic acid to produce PGE2. In response to various inflammatory stimuli, both NO and PGE2 interact with other chemokines and cytokines to generate ROS and RNS species, which are responsible for oxidative damage to the site of infection, despite their profound anti-inflammatory/antimicrobial activity. Especially in ocular pathologies, excess production of ROS and RNS increases cytotoxicity, causing tissue damage and if in cornea, loss of corneal clarity.[48]

In the current study, we found that GLY suppressed iNOS and COX-2 expression in human and murine Mϕ stimulated by LPS, TLR4-specific ultrapure LPS (latter used because it only interacts with TLR4), and 10 MOI of bacterial isolate KEI 1025. The latter provides evidence that GLY has a

broader effect on bacterial virulence factors and is not limited to affecting LPS alone. Differences in the effects of GLY between the 2 groups (Fig. 4A–D) suggested that GLY may affect HMGB1/TLR4 signaling. Moreover, GLY topical treatment after infection significantly reduced the production of ROS and RNS in the *P. aeruginosa*-infected cornea, with better disease outcome. Consistent with these findings, Vitali et al.[49] used LPS (not ultrapure)-stimulated Mϕ, and a mouse model of colitis and similarly showed that GLY inhibits the expression of iNOS and COX-2.

In addition to its anti-inflammatory/antimicrobial activity, GLY functions to bioenhance other drugs, including antimicrobials.[50–54] It does this due to its physiochemical properties, including its ability to increase membrane permeability and form micelle-like aggregates.[53,54] These features enhance the solubility, availability, and therapeutic efficacy of less soluble hydrophobic pharmaceutical compounds. In the present study, topical combined therapy at 6 h p.i. using TOB, an amphiphilic aminoglycoside antibiotic,[55] and GLY enhanced the therapeutic effects of the antibiotic and significantly reduced viable bacterial load compared with antibiotic alone. Unfortunately, we do not know the mechanism involved, but it is possible that GLY reduced TOB hydrophobicity.

Most relevant clinically, when similar treatment was delayed to 24 h p.i., the therapeutic efficacy of GLY together with TOB was again evident with improved disease clinical scores, reduced opacity, remarkably improved histopathology, reduced bacterial plate count, and reduction in expression of chemoattractant cytokines compared with all other treatments.

In summary, we provide evidence that GLY, FDA approved as a food supplement,[56] when given topically after infection improves disease outcome, regulates HMGB1-mediated inflammatory effects, bacterial viability, and is therapeutic in *P. aeruginosa* keratitis. It also significantly potentiates the effects of an antibiotic, TOB, by bioenhancing its effects even when treatment is delayed to 24 h p.i. Finally, *in vitro,* GLY modulates Mϕ release of oxidative stress-associated molecules not only in mouse but also in human cells, providing a tantalizing relevance to human treatment paradigms.

Acknowledgments

This work was supported by grants R01EY016058 and P30EY004068 from the National Eye Institute, National Institutes of Health and by a Research to Prevent Blindness unrestricted grant to the Department of Ophthalmology, Kresge Eye Institute.

Author Disclosure Statement

No competing financial interests exist.

References

1. Hazlett, L., Suvas, S., McClellan, S., and Ekanayaka, S. Challenges of corneal infections. *Expert Rev. Ophthalmol*. 11:285–297, 2016.
2. Pachigolla, G., Blomquist, P., and Cavanagh, H.D. Microbial keratitis pathogens and antibiotic susceptibilities: a 5-year review of cases at an urban county hospital in north Texas. *Eye Contact Lens*. 33:45–49, 2007.
3. Green, M., Apel, A., and Stapleton, F. Risk factors and causative organisms in microbial keratitis. *Cornea*. 27:22–27, 2008.
4. Lister, P.D., Wolter, D.J., and Hanson, N.D. Antibacterial-resistant *Pseudomonas aeruginosa*: clinical impact and complex regulation of chromosomally encoded resistance mechanisms. *Clin. Microbiol. Rev*. 22:582–610, 2009.
5. Wong, R.L., Gangwani, R.A., Yu, L.W., and Lai, J.S. New treatments for bacterial keratitis. *J. Ophthalmol*. 2012: 831502, 2012.
6. Andersson, U., and Tracey, K.J. HMGB1 is a therapeutic target for sterile inflammation and infection. *Annu. Rev. Immunol*. 29:139–162, 2011.
7. Wang, H., Bloom, O., Zhang, M., et al. HMG-1 as a late mediator of endotoxin lethality in mice. *Science*. 285:248–251, 1999.
8. Hazlett, L.D., McClellan, S.A., and Ekanayaka, S.A. Decreasing HMGB1 levels improves outcome of *Pseudomonas aeruginosa* keratitis in mice. *J. Rare Dis. Res. Treat*. 1:4, 2016.
9. McClellan, S., Jiang, X., Barrett, R., and Hazlett, L.D. High-mobility group box 1: a novel target for treatment of *Pseudomonas aeruginosa* keratitis. *J. Immunol*. 194:1776–1787, 2015.
10. Ekanayaka, S.A., McClellan, S.A., Barrett, R.P., Kharotia, S., and Hazlett, L.D. Glycyrrhizin reduces HMGB1 and bacterial load in *Pseudomonas aeruginosa* keratitis. *Invest. Ophthalmol. Vis. Sci*. 57:5799–5809, 2016.
11. Xue, H.Y., Liu, S., and Wong, H.L. Nanotoxicity: a key obstacle to clinical translation of siRNA-based nanomedicine. *Nanomedicine (Lond)*. 9:295–312, 2014.
12. Borna, H., Imani, S., Iman, M., and Azimzadeh Jamalkandi, S. Therapeutic face of RNAi: in vivo challenges. *Expert Opin. Biol. Ther*. 15:269–285, 2015.
13. O'Brien, T.P. Management of bacterial keratitis: beyond exorcism towards consideration of organism and host factors. *Eye (Lond)*. 17:957–974, 2003.
14. Baum, J., and Barza, M. Topical vs subconjunctival treatment of bacterial corneal ulcers. *Ophthalmology*. 90:162–168, 1983.
15. Leibowitz, H.M., Ryan, W.J., Jr., and Kupferman, A. Route of antibiotic administration in bacterial keratitis. *Arch. Ophthalmol*. 99:1420–1423, 1981.
16. McClellan, S.A., Ekanayaka, S.A., Li, C., et al. Thrombomodulin protects against bacterial keratitis, is anti-inflammatory, but not angiogenic. *Invest. Ophthalmol. Vis. Sci*. 56:8091–8100, 2015.
17. Gokhale, N.S. Medical management approach to infectious keratitis. *Indian J. Ophthalmol*. 56:215–220, 2008.
18. Carion, T.W., McWhirter, C.R., Grewal, D.K., and Berger, E.A. Efficacy of VIP as treatment for bacteria-induced keratitis against multiple *Pseudomonas aeruginosa* strains. *Invest. Ophthalmol. Vis. Sci*. 56:6932–6940, 2015.
19. Hazlett, L.D., Moon, M.M., Strejc, M., and Berk, R.S. Evidence for N-acetylmannosamine as an ocular receptor for *P. aeruginosa* adherence to scarified cornea. *Invest. Ophthalmol. Vis. Sci*. 28:1978–1985, 1987.
20. Mencucci, R., Favuzza, E., and Menchini, U. Assessment of the tolerability profile of an ophthalmic solution of 5% glycyrrhizin and copolymer PEG/PPG on healthy volunteers and evaluation of its efficacy in the treatment of moderate to severe blepharitis. *Clin. Ophthalmol*. 7:1403–1410, 2013.
21. Mercuri, L. Pharmaceutical composition based on glycyrrhizin and eg56 polymer for the preparation of anti-inflammatory products. Google Patents; 2011.
22. Williams, R.N., Paterson, C.A., Eakins, K.E., and Bhattacherjee, P. Quantification of ocular inflammation: evaluation of polymorphonuclear leucocyte infiltration by measuring myeloperoxidase activity. *Curr. Eye Res*. 2:465–470, 1982.
23. Huang, X., Du, W.J., McClellan, S.A., Barrett, R.P., and Hazlett, L.D. TLR4 is required for host resistance in

Pseudomonas aeruginosa keratitis. *Invest. Ophthalmol. Vis. Sci*. 47:4910–4916, 2006.
24. Fortier, A.H., and Falk, L.A. Isolation of murine macrophages. *Curr. Protoc. Immunol*. Chapter 14:Unit 14 11, 2001.
25. Hazlett, L.D., McClellan, S.A., Barrett, R.P., et al. IL-33 shifts macrophage polarization, promoting resistance against *Pseudomonas aeruginosa* keratitis. *Invest. Ophthalmol. Vis. Sci*. 51:1524–1532, 2010.
26. Heid, C.A., Stevens, J., Livak, K.J., and Williams, P.M. Real time quantitative PCR. *Genome Res*. 6:986–994, 1996.
27. Vazirani, J., Wurity, S., and Ali, M.H. Multidrug-resistant *Pseudomonas aeruginosa* keratitis risk factors, clinical characteristics, and outcomes. *Ophthalmology*. 122:2110–2114, 2015.
28. Murugan, N., Malathi, J., Umashankar, V., and Madhavan, H.N. Unraveling genomic and phenotypic nature of multidrug-resistant (MDR) *Pseudomonas aeruginosa* VRFPA04 isolated from keratitis patient. *Microbiol. Res*. 193:140–149, 2016.
29. Wang, W., Zhao, F., Fang, Y., et al. Glycyrrhizin protects against porcine endotoxemia through modulation of systemic inflammatory response. *Crit. Care*. 17:R44, 2013.
30. Liu, Y., Xiang, J., Liu, M., et al. Protective effects of glycyrrhizic acid by rectal treatment on a TNBS-induced rat colitis model. *J. Pharm. Pharmacol*. 63:439–446, 2011.
31. Ni, Y.F., Kuai, J.K., Lu, Z.F., et al. Glycyrrhizin treatment is associated with attenuation of lipopolysaccharide-induced acute lung injury by inhibiting cyclooxygenase-2 and inducible nitric oxide synthase expression. *J. Surg. Res*. 165:e29–e35, 2011.
32. Gong, G., Xiang, L., Yuan, L., et al. Protective effect of glycyrrhizin, a direct HMGB1 inhibitor, on focal cerebral ischemia/reperfusion-induced inflammation, oxidative stress, and apoptosis in rats. *PLoS One*. 9:e89450, 2014.
33. Arase, Y., Ikeda, K., Murashima, N., et al. The long term efficacy of glycyrrhizin in chronic hepatitis C patients. *Cancer*. 79:1494–1500, 1997.
34. Mollica, L., De Marchis, F., Spitaleri, A., et al. Glycyrrhizin binds to high-mobility group box 1 protein and inhibits its cytokine activities. *Chem. Biol*. 14:431–441, 2007.
35. Ogiku, M., Kono, H., Hara, M., Tsuchiya, M., and Fujii, H. Glycyrrhizin prevents liver injury by inhibition of high-mobility group box 1 production by Kupffer cells after ischemia-reperfusion in rats. *J. Pharmacol. Exp. Ther*. 339:93–98, 2011.
36. Zhang, J., Wu, Y., Weng, Z., et al. Glycyrrhizin protects brain against ischemia-reperfusion injury in mice through HMGB1-TLR4-IL-17A signaling pathway. *Brain Res*. 1582:176–186, 2014.
37. Xiang, K., Cheng, L., Luo, Z., et al. Glycyrrhizin suppresses the expressions of HMGB1 and relieves the severity of traumatic pancreatitis in rats. *PLoS One*. 9:e115982, 2014.
38. Shen, L., Cui, Z., Lin, Y., et al. Anti-inflammative effect of glycyrrhizin on rat thermal injury via inhibition of high-mobility group box 1 protein. *Burns*. 41:372–378, 2015.
39. Zhao, F., Fang, Y., Deng, S.X., et al. Glycyrrhizin protects rats from sepsis by blocking HMGB1 signaling. *Biomed. Res. Int*. 2017:9719647, 2017.
40. van Beijnum, J.R., Buurman, W.A., and Griffioen, A.W. Convergence and amplification of toll-like receptor (TLR) and receptor for advanced glycation end products (RAGE) signaling pathways via high mobility group B1 (HMGB1). *Angiogenesis*. 11:91–99, 2008.
41. Sims, G.P., Rowe, D.C., Rietdijk, S.T., Herbst, R., and Coyle, A.J. HMGB1 and RAGE in inflammation and cancer. *Annu. Rev. Immunol*. 28:367–388, 2010.
42. Taniguchi, N., Kawahara, K., Yone, K., et al. High mobility group box chromosomal protein 1 plays a role in the pathogenesis of rheumatoid arthritis as a novel cytokine. *Arthritis Rheum*. 48:971–981, 2003.
43. Hazlett, L.D. Corneal response to *Pseudomonas aeruginosa* infection. *Prog. Retin. Eye Res*. 23:1–30, 2004.
44. Berthelot, F., Fattoum, L., Casulli, S., et al. The effect of HMGB1, a damage-associated molecular pattern molecule, on polymorphonuclear neutrophil migration depends on its concentration. *J. Innate Immun*. 4:41–58, 2012.
45. Ding, H.S., Yang, J., Gong, F.L., et al. High mobility box 1 mediates neutrophil recruitment in myocardial ischemia-reperfusion injury through toll like receptor 4-related pathway. *Gene*. 509:149–153, 2012.
46. Lin, M., Carlson, E., Diaconu, E., and Pearlman, E. CXCL1/KC and CXCL5/LIX are selectively produced by corneal fibroblasts and mediate neutrophil infiltration to the corneal stroma in LPS keratitis. *J. Leukoc. Biol*. 81:786–792, 2007.
47. Tilley, S.L., Coffman, T.M., and Koller, B.H. Mixed messages: modulation of inflammation and immune responses by prostaglandins and thromboxanes. *J. Clin. Invest*. 108:15–23, 2001.
48. Cejka, C., and Cejkova, J. Oxidative stress to the cornea, changes in corneal optical properties, and advances in treatment of corneal oxidative injuries. *Oxid. Med. Cell Longev*. 2015:591530, 2015.
49. Vitali, R., Palone, F., Pierdomenico, M., et al. Dipotassium glycyrrhizate via HMGB1 or AMPK signaling suppresses oxidative stress during intestinal inflammation. *Biochem. Pharmacol*. 97:292–299, 2015.
50. Dudhatra, G.B., Mody, S.K., Awale, M.M., et al. A comprehensive review on pharmacotherapeutics of herbal bioenhancers. *ScientificWorldJournal*. 2012:637953, 2012.
51. Tolstikova, T.G., Khvostov, M.V., and Bryzgalov, A.O. The complexes of drugs with carbohydrate-containing plant metabolites as pharmacologically promising agents. *Mini Rev. Med. Chem*. 9:1317–1328, 2009.
52. Polyakov, N., and Leshina, T. Glycyrrhizic acid as a novel drug delivery vector: synergy of drug transport and efficacy. *Open Conf. Proc. J*. 2:64–72, 2011.
53. Selyutina, O.Y., Polyakov, N.E., Korneev, D.V., and Zaitsev, B.N. Influence of glycyrrhizin on permeability and elasticity of cell membrane: perspectives for drugs delivery. *Drug Deliv*. 23:858–865, 2016.
54. Kornievskaya, V.S., Kruppa, A.I., and Leshina, T.V. NMR and photo-CIDNP investigations of the glycyrrhizinic acid micelles influence on solubilized molecules. *J. Incl. Phenom. Macrocycl. Chem.* 60:123–130, 2008.
55. Dhondikubeer, R., Bera, S., Zhanel, G.G., and Schweizer, F. Antibacterial activity of amphiphilic tobramycin. *J. Antibiot. (Tokyo)*. 65:495–498, 2012.
56. Omar, H.R., Komarova, I., El-Ghonemi, M., et al. Licorice abuse: time to send a warning message. *Ther. Adv. Endocrinol. Metab*. 3:125–138, 2012.

Received: August 16, 2017
Accepted: November 9, 2017

Address correspondence to:
Dr. Linda D. Hazlett
Department of Anatomy and Cell Biology
Wayne State University School of Medicine
540 East Canfield Avenue
Detroit, MI 48201

E-mail: lhazlett@med.wayne.edu